

A peer-reviewed version of this preprint was published in PeerJ on 4 April 2018.

[View the peer-reviewed version](https://peerj.com/articles/4603) (peerj.com/articles/4603), which is the preferred citable publication unless you specifically need to cite this preprint.

Escobar-Flores JG, Lopez-Sanchez CA, Sandoval S, Marquez-Linares MA, Wehenkel C. 2018. Predicting *Pinus monophylla* forest cover in the Baja California Desert by remote sensing. PeerJ 6:e4603
<https://doi.org/10.7717/peerj.4603>

1 Predicting *Pinus monophylla* forest cover in the Baja 2 California Desert by remote sensing

3 Jonathan G. Escobar-Flores ¹, Carlos A. López-Sánchez ², Sarahi Sandoval ³, Marco A. Márquez-Linares
4 ¹, Christian Wehenkel ²

5 ¹ Instituto Politécnico Nacional. Centro Interdisciplinario De Investigación para el Desarrollo Integral
6 Regional, Unidad Durango., Durango, México

7 ² Instituto de Silvicultura e Industria de la Madera, Universidad Juárez del Estado de Durango, Durango,
8 México

9 ³ CONACYT - Instituto Politécnico Nacional. CIIDIR. Unidad Durango. Durango, México

10

11 Corresponding author:

12 Christian Wehenkel ²

13 Km 5.5 Carretera Mazatlán, Durango, 34120 Durango, México

14 Email address: wehenkel@ujed.mx

15

16

17 ABSTRACT

18 **Background.** The Californian single-leaf pinyon (*Pinus monophylla* var. *californiarum*), a
19 subspecies of the single-leaf pinyon (the world's only 1-needled pine), inhabits semi-arid zones of
20 the Mojave Desert (southern Nevada and southeastern California, US) and also of northern Baja
21 California (Mexico). This tree is distributed as a relict subspecies, at elevations of between 1,010
22 and 1,631 m in the geographically isolated arid Sierra La Asamblea (Baja California, Mexico), an
23 area characterized by mean annual precipitation levels of between 184 and 288 mm. The aim of
24 this research was i) to estimate the distribution of *P. monophylla* var. *californiarum* in Sierra La
25 Asamblea by using Sentinel-2 images, and ii) to test and describe the relationship between the
26 distribution of *P. monophylla* and five topographic and 18 climate variables. We hypothesized that
27 i) Sentinel-2 images can be used to predict the *P. monophylla* distribution in the study site due to

28 the finer resolution (x3) and greater number of bands (x2) relative to Landsat-8 data, which is
29 publically available free of charge and has been demonstrated to be useful for estimating forest
30 cover, and ii) the topographical variables aspect, ruggedness and slope are particularly important
31 because they represent important microhabitat factors that can determine the sites where conifers
32 can become established and persist. **Methods.** An atmospherically corrected a 12-bit Sentinel-2A
33 MSI image with ten spectral bands in the visible, near infrared, and short-wave infrared light region
34 was used in combination with the normalized differential vegetation index (NDVI). Supervised
35 classification of this image was carried out using a backpropagation-type artificial neural network
36 algorithm (BPNN). Stepwise multivariate binominal logistical regression and Random Forest
37 classification including cross valuation (10-fold) were used to model the associations between
38 presence/absence of *P. monophylla* and the five topographical and 18 climate variables. **Results.**
39 Using supervised classification of Sentinel-2 satellite images, we estimated that *P. monophylla*
40 covers $6,653 \pm 319$ hectares in the isolated Sierra La Asamblea. The NDVI was one of the variables
41 that contributed most to the prediction and clearly separated the forest cover ($NDVI > 0.35$) from
42 the other vegetation cover ($NDVI < 0.20$). Ruggedness was the most influential environmental
43 predictor variable, indicating that the probability of occurrence of *P. monophylla* was higher than
44 50% when the degree of ruggedness TRI was greater than 17.5 m. The probability of occurrence
45 of the species decreased when the mean temperature in the warmest month increased from 23.5 to
46 25.2 °C. **Discussion.** The accuracy of classification was similar to that reported in other studies
47 using Sentinel-2A MSI images. Ruggedness is known to create microclimates and provides shade
48 that minimizes evapotranspiration from pines in desert environments. Identification of the *P.*
49 *monophylla* stands in Sierra La Asamblea as the most southern populations represents an

50 opportunity for research on climatic tolerance and community responses to climate variability and
51 change.

52 INTRODUCTION

53 The Californian single-leaf pinyon (*Pinus monophylla* var. *californiarum*), a subspecies of the
54 single-leaf pinyon (the world's only 1-needled pine), inhabits semi-arid zones of the Mojave Desert
55 (southern Nevada and southeastern California, US) and also of northern Baja California (BC)
56 (Mexico). It is both cold-tolerant and drought-resistant and is mainly differentiated from the typical
57 subspecies *Pinus monophylla* var. *monophylla* by a larger number of leaf resin canals and longer
58 fascicle-sheath scales (Bailey, 1987). This subspecies was first reported in BC in 1767 (Bullock et
59 al., 2006). The southernmost record of *P. monophylla* var. *californiarum* in America was
60 previously in BC, 26-30 miles north of Punta Prieta, at an elevation of 1,280 m (longitude -
61 114°.155; latitude 29°.070, catalogue number ASU 0000235), and the type specimen is held in the
62 Arizona State University Vascular Plant Herbarium.

63 This tree is distributed as a relict subspecies in the geographically isolated Sierra La Asamblea, at
64 a distance of 196 km from the Southern end of the Sierra San Pedro Martir and at elevations of
65 between 1,010 and 1,631 m (Moran, 1983) in areas with mean annual precipitation levels of
66 between 184 and 288 mm (Roberts & Ezcurra, 2012). The Californian single-leaf pinyon grows
67 together with up to about 86 endemic plant species, although the number of species decreases from
68 north to south (Bullock et al., 2008).

69 Adaptation of *P. monophylla* var. *californiarum* to arid ecosystems enables the species to survive
70 annual precipitation levels of less than 150 mm. In fact, seeds of this variety survive well under

71 shrubs such as *Quercus spp.* and *Arctostaphylos spp.*, a strategy that enables the pines to widen
72 their distribution, as has occurred in the great basin in California (Callaway et al., 1996; Chambers,
73 2001), and for them to occupy desert zones such as Sierra de la Asamblea. Despite the importance
74 of this relict pine species, its existence is not considered in most forest inventories in Mexico
75 (CONABIO, 2017).

76 Remote sensing with Landsat images has been demonstrated to be useful for estimating forest
77 cover; the The Landsat-8 satellite has sensors (7 bands) that can be used to analyze vegetation at a
78 spatial resolution of 30 m (Madonsela et al., 2017). However, the European Space Agency's
79 Copernicus program has made Sentinel-2 satellite images available to the public free of charge.
80 The spatial resolution (10 m is pixel) of the images is three times finer that of Landsat images, thus
81 increasing their potential for predicting and differentiating types of vegetation cover (Drush et al.,
82 2012; Borrás et al., 2017). The Sentinel-2 has 13 bands, of which 10 provide high-quality
83 radiometric images of spatial resolution 10 to 20 m in the visible and infrared regions of the
84 electromagnetic spectrum. These images are therefore ideal for land classification (ESA, 2017).

85 The aim of this research was i) to estimate the distribution of *Pinus monophylla* var. *californiarum*
86 in Sierra La Asamblea, Baja California (Mexico) by using Sentinel-2 images, and ii) to test and
87 describe the relationship between this distribution of *P. monophylla* and five topographic and 18
88 climate variables. We hypothesized that i) the Sentinel-2 images can be used to accurately predict
89 the *P. monophylla* distribution in the study site due to finer resolution (x3) and greater number of
90 bands (x2) than in Landsat-8 data, and ii) the topographical variables aspect, ruggedness and slope
91 are particularly influential because they represent important microhabitat factors that can
92 determine where conifers can become established and persist (Marston, 2010).

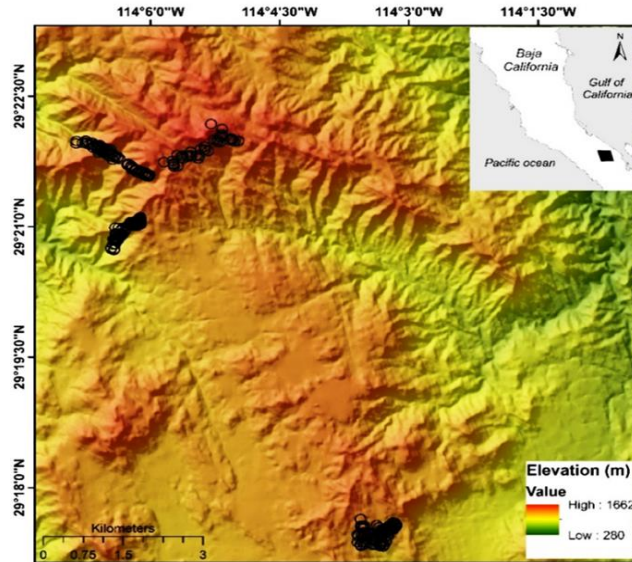
93 MATERIALS AND METHODS

94 Study area

95 Sierra La Asamblea is located in Baja California's central desert (-114° 9' W 29° 19' N, elevation
96 range 280-1,662 m, Fig. 1). The climate in the area is arid, with maximum temperatures of 40° C
97 in the summer (Garcia, 1998). The sierra is steeper on the western slopes, with an average incline
98 of 35°, and with numerous canyons with occasional springs and oases. Valleys and plateaus are
99 common in the proximity of the Gulf of California. Granite rocks occur south of the sierra and
100 meta-sedimentary rocks along the north and southeast of the slopes. The predominant type of
101 vegetation is xerophilous scrub, which is distributed at elevations ranging from 200 to 1,000 m.
102 Chaparral begins at an altitude of 800 m, and representative specimens of *Adenostoma*
103 *fasciculatum*, *Ambrosia ambrosioides*, *Dalea bicolor orcuttiana* *Quercus tuberculata*, *Juniperus*
104 *california* and *Pinus monophylla* are also present at elevations above 1,000 m. Populations of the
105 endemic palm tree *Brahea armata* also occur in the lower parts of the canyons with superficial
106 water flow and through the rocky granite slopes (Bullock et al., 2006).

107
108 **Figure 1.** Map of Sierra La Asamblea. The black circles indicate georeferenced sites occupied by
109 *Pinus monophylla*.

110



111

112 Datasets

113 Sentinel-2

114 The Sentinel-2A multispectral instrument (MSI) L1C dataset, acquired on 11 October 2016, in the
115 trajectory of coordinates latitude $29^{\circ}.814$, longitude $114^{\circ}.93$, was downloaded from the US
116 Geological Survey (USGS) Global Visualization Viewer at <http://glovis.usgs.gov/>. The 12-bit
117 Sentinel-2A MSI image has 13 spectral bands in the visible, NIR, and SWIR wavelength regions
118 with spatial resolutions of 10-60 m. However, band one, used for studies of coastal aerosols, and
119 bands nine and ten, applied for respectively water vapour correction and cirrus detection, were not
120 used in this study (ESA, 2017). Hence, the data preparation involved four bands at 10 m and the
121 resampling of the six S2 bands acquired at 20 m to obtain a layer stack of 10 spectral bands at 10
122 m (Table 1) using the ESA's Sentinel-toolbox ESA Sentinel Application Platform (SNAP) and
123 then converted to ENVI format.

124 Because atmospherically improved images are essential to enable assessment of spectral indices
125 with spatial reliability and product comparison, Level-1C data were converted to Level-2A

126 (Bottom of Atmosphere -BOA- reflectance) by taking into account the effects of aerosols and
 127 water vapour on reflectance (Radoux et al., 2016). The corrections were made using the Sen2Cor
 128 tool (Telespazio VEGA Deutschland GmbH, 2016) for Sentinel-2 images.

129 **Table 1.** Sentinel-2 spectral bands used to predict the *Pinus monophylla* forest cover

Bands	Central wave length (µm)	Resolution (m)
Band 2–Blue	0.490	10
Band 3 –Green	0.560	10
Band 4 – Red	0.665	10
Band 5- Vegetation red edge	0.705	20
Band 6– Vegetation red edge	0.740	20
Band 7– Vegetation red edge	0.783	20
Band 8- NIR	0.842	10
Band 8A– Vegetation red edge	0.865	20
Band 11 –SWIR	1.610	20
Band 12 –SWIR	2.190	20

130
 131 The following equation was used to calculate the normalized difference vegetation index (NDVI):
 132 $NDVI = (NIR - R) / (NIR + R)$, where NIR is the near infrared light (band) reflected by the
 133 vegetation, and R is the visible red light reflected by the vegetation (Rouse et al., 1974). The NDVI
 134 is useful for discriminating the layers of temperate forest from scrub and chaparral. Areas occupied
 135 by large amounts of unstressed green vegetation will have values much higher than 0 and areas
 136 with no vegetation will have values close to 0 and, in some cases, negative values (Pettorelli,
 137 2013). The NDVI image was combined with the previously described multi spectral bands.

138 Environmental variables

139 Tree species distribution is generally modulated by hydroclimate and topographical variables
 140 (Elliot et al., 2005; Decastilho et al., 2006), which can be estimated from digital terrain models
 141 (DTM) (Osem et al., 2005; Spasojevic et al., 2016). A DTM was obtained by using tools available

142 from the Instituto Nacional de Estadística y Geografía
143 (<http://www.inegi.org.mx/geo/contenidos/datosrelieve>) with a spatial resolution of 15 m. The DTM
144 was processed with the QGIS (QGIS Development Team, 2016), using *Terrain analysis* tools,
145 elevation, slope and aspect (Table 2).

146 The ruggedness was estimated using two indexes: i) the terrain ruggedness index (TRI) of Riley
147 et al. (1999) and ii) a vector ruggedness measure (VRM), both implemented in QGIS (QGIS
148 Development Team, 2016). The TRI computes the values for each grid cell of a DEM. This
149 calculates the sum change in elevation between a grid cell and its eight-neighbor grid cell. VRM
150 incorporates the heterogeneity of both slope and aspect. This measure of ruggedness uses 3-
151 dimensional dispersion of vectors normal to planar facets on landscape. This index lacks units and
152 ranges from 0 (indicating a totally flat area) to 1 (indicating maximum ruggedness) (Sappington et
153 al., 2007).

154 In addition, 18 climate variables with a 30-arc second resolution (approximate 800 meters) (Table
155 2) were obtained from a national database managed by the University of Idaho
156 (<http://charcoal.cnre.vt.edu/climate>) and which requires point coordinates (latitude, longitude and
157 elevation) as the main inputs (Rehfeldt, 2006; Rehfeldt et al., 2006). These variables are frequently
158 used to study the potential effects of global warming on forests and plants in Western North
159 America and Mexico (Sáenz-Romero et al., 2010; Silva-Flores et al., 2014).

160

161

162

163 **Table 2.** Topographical and climatic variables considered in the study

Variable	Abbreviation	Units	Mean	SD	Max	Min
Ruggedness	IRT	m	20.33	6.66	35.90	4.69
Ruggedness VRM	VRM	NA	0.005	0.007	0.13	0
Slope	S	°	28.38	8.92	48.34	3.42
Aspect *	A	°	190.51	68.72	350.44	20.55
Elevation *	E	m	1302.41	124.96	1631	1010
Mean annual temperature *	MAT	°C	16.57	0.38	17.4	15.5
Mean annual precipitation *	MAP	mm	229.56	19.95	288	184
Growing season precipitation, April-September *	GSP	mm	79.08	9.60	108	57
Mean temperature in the coldest month *	MTCM	°C	10.85	0.37	11.7	9.8
Minimum temperature in the coldest month *	MMIN	°C	3.42	0.41	4.3	2.3
Mean temperature in the warmest month	MTWM	°C	24.52	0.31	25.2	23.5
Maximum temperature in the warmest month	MMAX	°C	34.10	0.31	34.7	33.1
Julian date of the last freezing data of spring *	SDAY	Days	82.57	7.86	106	60
Julian date of the first freezing data of autumn *	FDAY	Days	331.28	2.62	339	324
Length of the frost-free period *	FFP	Days	259.22	8.36	285	240
Degree days > 5°C *	DD5	Days	4245.26	137.52	4550	3852
Degree days > 5°C accumulating within the frost-free period *	GSDD5	Days	3491.82	164.76	3944	2995
Julian date when the sum degree days > 5°C reaches 100 *	D100	Days	17.07	1.10	20	15
Degree days < 0 °C *	DD0	Days	0	0	0	0
Minimum degree days < 0 °C *	MMINDD0	Days	8.07	20.29	145	45
Spring precipitation	Sprp	mm	7.54	0.71	10	6
Summer precipitation *	Smrp	mm	43.74	6.29	62	29
Winter precipitation *	Winp	mm	110.93	7.93	133	93

164 * Variables for which no significant difference between the medians was obtained after
 165 Bonferroni correction ($\alpha = 0.0005$) were excluded from further analysis.

166

167 **Pixel-based classification**

168 **Classification method**

169 Pixel-based classification was carried out in order to identify four different types of land cover in
170 the study area (*P. monophylla*, scrub, chaparral and no apparent vegetation). A supervised
171 classification approach with a backpropagation-type artificial neural network (BPNN) (SNAP,
172 2017) was applied. BPNN is widely used because of its structural simplicity and robustness in
173 modelling non-linear relationships. In this study, the BPNN comprises a set of three layers (raster):
174 an input layer, a hidden layer and an output layer (Richards, 1993). Each layer consists of a series
175 of parallel processing elements (neurons or nodes). Each node in a layer is linked to all nodes in
176 the next layer (Guo et al., 2013).

177 The first step in BPNN supervised classification is to enter the input layer, which in this study
178 corresponded to the values of the pixels of ten Sentinel-2 bands and of the NDVI image. Weights
179 were then assigned to the BPNN to produce analytical predictions from the input values. These
180 data were contrasted with the category to which each training pixel belongs, corresponding to
181 Georeferenced sites (Datum WGS-84, 11N) obtained in the field in October 2014 and October
182 2015.

183 A stratified random sampling method (Olofsson et al., 2013) was used to generate the reference
184 data in QGIS software (QGIS Development Team 2016). A total of 4017 random points were
185 sampled, with at least 400 points for each class (Goodchild et al., 1994). The following classes
186 were considered: i) *P. monophylla*, 502 sites, ii) scrub, 563 sites, iii) chaparral, 419 sites, and iv)
187 no apparent vegetation, 419 sites. Class discrimination processes occurred in the hidden layer and
188 the synapses between the layers were estimated by an activation function. We used a logistic

189 function and training rate of 0.20, previously applied to land cover classification (Hepner et al.,
190 1990; Richards, 1993; Braspenning & Thuijisman, 1995). Learning occurs by adjusting the
191 weights in the node to minimize the difference between the output node activation, and BPNN
192 then calculates the error at each iteration with root square error (RMS). The output layer comprised
193 four neurons representing the four target classes of land cover (*P. monophylla*, scrub, chaparral
194 and no apparent vegetation).

195 **Validation**

196 The BPNN classification was cross-validated (10-fold) using a confusion matrix, which is a table
197 that compares the reference data and the classification results. The confusion matrix was also used
198 to estimate the overall accuracy (the proportion of the area mapped correctly), user accuracy
199 (proportion of the area mapped as a particular category that is actually that category) and producer
200 accuracy (proportion of the area that is a particular category on the ground that is also mapped as
201 that category) (Congalton, 1991). We estimated the uncertainty of the classification through
202 estimated error matrix with 95% confidence intervals. We then generated a map from the results
203 of the probability of class assignment. Finally, we estimated the area of *P. monophylla* and estimate
204 the standard error, error-adjusted and 95% confidence intervals proposed by Olofsson et al. (2013).
205 The accuracy of classification was also estimated using the Kappa (K) coefficient. The K
206 coefficient is often used as an overall measure of accuracy (Abraira, 2001). This coefficient takes
207 values of between 0 and 1, where values close to one indicate a high degree of agreement between
208 classes and observations, and a value of 0 suggests that the observed agreement is random (Abraira,
209 2001). However, the use of K is controversial because i) K would underestimate the probability
210 that a randomly selected pixel is correctly classified, ii) K is highly correlated with overall accuracy
211 so reporting Kappa is redundant for overall accuracy (Olofsson et al., 2014).

212 **Relationship between presence of *P. monophylla* and environmental variables**

213 To model and test the association between presence/absence of *P. monophylla* in the study area
214 and topographical or climate variables, a Kruskal-Wallis test was used to estimate the difference
215 in the median values in relation to presence and absence of *P. monophylla*. All variables for which
216 no significant difference between the median values was predicted after Bonferroni correction (α
217 = 0.0005) were excluded from further analysis. The collinearity between the variables with a
218 significant difference between the medians of presence and absence was estimated using the
219 Spearman correlation coefficient (r_s). When the r_s value for the difference between two variables
220 was greater than 0.7, only the variable with the lowest p value in the Kruskal-Wallis test was used
221 in the multivariate models (as reported by Salas et al., 2017 and Shirk et al., 2018). Finally,
222 stepwise multivariate binominal logistical regression and Random Forest classification including
223 cross valuation (10-fold) were used to model the associations between presence/absence of *P.*
224 *monophylla* and the most important topographical and climate variables (Shirk et al., 2018).

225 Regression and classification including cross-validations were carried out using the trainControl,
226 train, glm (family = "binomial") and rf functions, as well as the "randomForest" and "caret"
227 packages (Venables and Ripley, 2002) in R (version 3.3.2) (Development Core Team, 2017). The
228 goodness-of-fit of the logistical regression model was evaluated using the Akaike information
229 criterion (AIC), root-mean-square error (RMSE) and residual deviance. Validation of the
230 randomForest model was performed using under the curve (AUC; Fawcett, 2006), True Skill
231 Statistic (TSS; Allouche et al., 2006), Kappa (Abraira, 2001), specificity and sensitivity.

232 **RESULTS**233 **Pixel-based classification**

234 We estimated the area of *P. monophylla* cover of $6,653 \pm 319$ hectares in Sierra de la Asamblea,
 235 Baja California, Mexico. The supervised classification with BPNN yielded predictions with an
 236 overall accuracy of identification of 87.74% (Table 3). This level of accuracy was estimated in the
 237 32 interactions with 0.04 RMS training. The proportion of omission errors in the pine class was
 238 only 12.42%, *i.e.* 87.58% of the pixels were correctly classified. The chaparral class had the larger
 239 proportion of omission errors (27.65%) (Fig. 2; Fig. 3). The value of NDVI in the *P. monophylla*
 240 forest fluctuated between 0.30 and 0.41, and in chaparral between 0.24 and 0.28. The lowest values
 241 of NDVI corresponded to scrub vegetation, with values between 0.10 and 0.15.

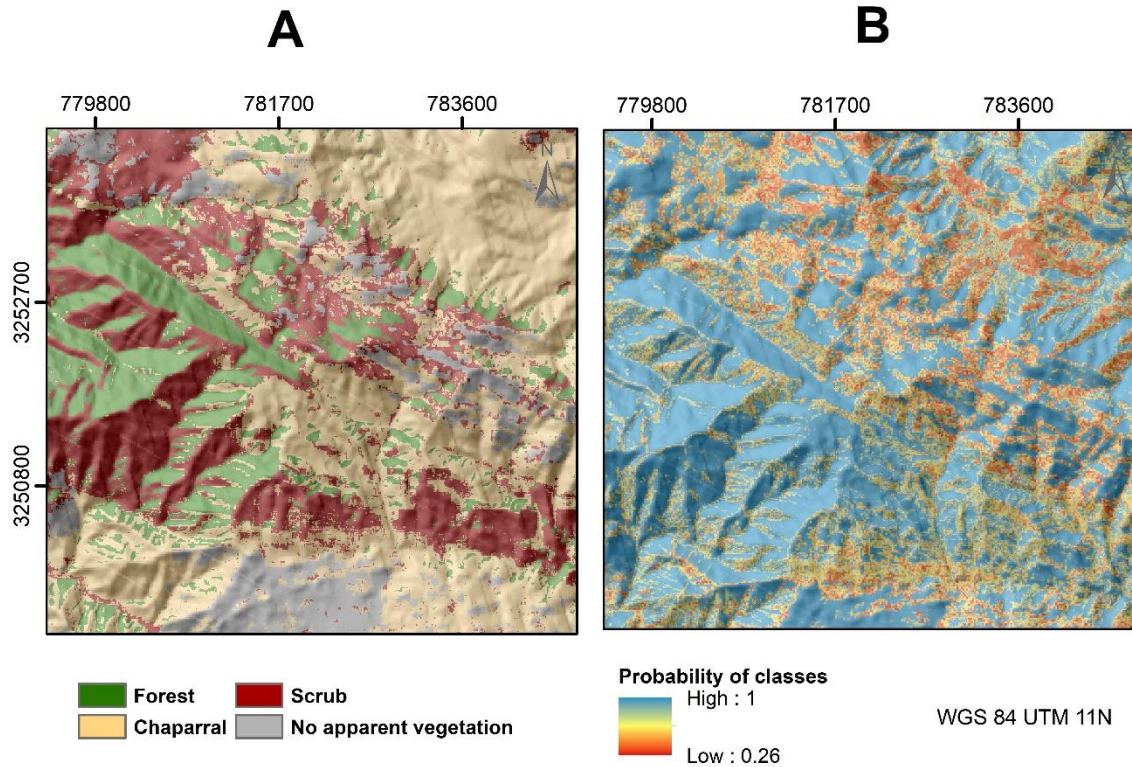
242 **Table 3.** Estimated error matrix based of sample counts expressed as the estimated area
 243 proportions (W_i). Accuracy measures are presented with a 95% confidence interval. Map
 244 categories are the rows while the reference categories are the columns.

Classification data	P	S	C	WV	Total	W_i	User's	Producer's	Overall
P	522	0	14	0	536	0.169	0.974±0.07	0.790±0.04	0.877±0.01
S	24	619	119	2	764	0.387	0.810±0.02	1.000	
C	50	0	348	7	405	0.258	0.859±0.01	0.752±0.07	
WV	0	0	20	418	438	0.186	0.954±0.002	0.970±0.02	
Total	596	619	501	427	2,143	1			

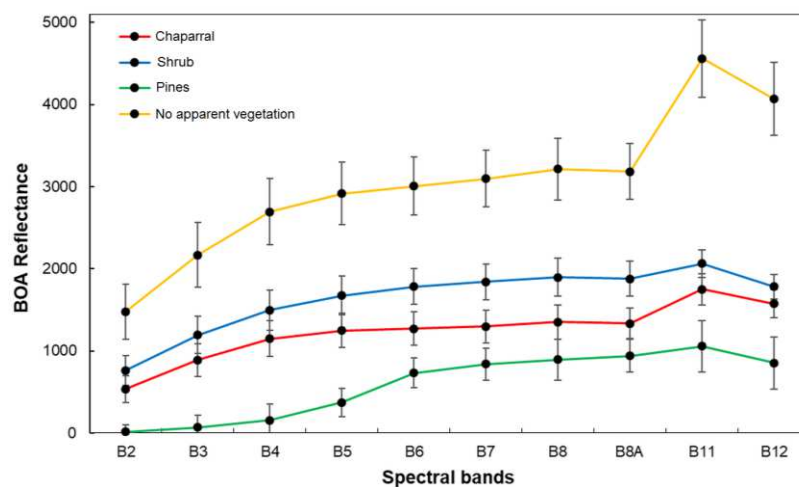
245 * P = *Pinus monophylla*; S = Shrub; C = Chaparral; WV= Without Vegetation; W_i = estimated
 246 area proportions.

247

248 **Figure 2.** (A) Estimated land cover classes using BPNN classification in Sierra La Asambla. (B)
 249 Probability map of class assignment.



251 **Figure 3.** Spectral signatures of cover vegetation in Sierra La Asamble, Baja California.



253 Relationship between presence of *P. monophylla* and environmental variables

254 The Kruskal-Wallis test indicated that the median values for ruggedness TRI ($p < 2.1 \times 10^{-16}$), slope
255 ($p < 2.2 \times 10^{-16}$), ruggedness VRM ($p = 4.9 \times 10^{-9}$), MTWM ($p = 0.000014$), MMAX ($p = 0.000048$)
256 and SPRP ($p = 0.00037$) were most variable between sites in which *P. monophylla* was present
257 and absent. The variable slope was closely correlated with ruggedness as well as with MMAX and
258 MTWM ($r_s > 0.7$). The p_{slope} of the Kruskal-Wallis test was larger than $p_{\text{ruggedness}}$ and p_{MMAX} was
259 larger than p_{MTWM} . Slope and MMAX were therefore excluded from the multivariate model
260 analysis. The stepwise multivariate binominal logistical and Random Forest models showed that
261 the “presence of *P. monophylla*” model included the independent variables ruggedness, ruggedness
262 VRM and average temperature in the warmest month (MTWM) (Table 4).

263 The ruggedness factor was the most influential predictor variable and indicated that the probability
264 of *P. monophylla* occurrence was larger than 50% when the degree of ruggedness TRI was higher
265 than 17.5 m (Table 4). The ruggedness VRM also indicated that a minimum change in roughness
266 increases the probability of presence of the pine. The probability of occurrence of *Pinus*
267 *monophylla* decreased when MTWM increased from 23.5 to 25.2 °C (Table 5). After cross
268 validation (10-fold), the Random Forest model revealed that the variables ruggedness TRI,
269 ruggedness VRM and MTWM yielded a high correlation for their ability to predict presence of the
270 *P. monophylla* (AUC = 0.920, TSS = 0.69, Kappa = 0.691). The sensitivity was 0.812 and
271 specificity was 0.878.

272 **Table 4.** Results of the multivariate binomial logistic regression model (AIC = 601.8; residual
273 deviance= 593.85 on 588 degrees of freedom), TRI = terrain ruggedness index, VRM = vector
274 ruggedness measure, MTWM = mean temperature in the warmest month.

Variable	Estimate	Std. Error	Z value	Pr(> z)
Intercept	25.351	8.895	2.850	0.0044
MTWM	-1.159	0.362	-3.201	0.0014
Roughness TRI	0.178	0.015	11.200	< 2e-16
Roughness VRM	28.476	13.847	2.056	0.0397

275

276 **DISCUSSION**277 ***Pixel-based classification***

278 Predicting the presence of pine forest by using BPNN proved feasible. The NDVI was one of the
 279 variables that contributed to the prediction and clearly separated forest cover ($NDVI > 0.35$) from
 280 the other types of vegetation cover ($NDVI < 0.20$). The overall accuracy of classification ($K =$
 281 0.87) was similar to that reported in other studies using Sentinel-2A MSI images; for example,
 282 Immitzer et al., (2016) reported a K of 0.85 for tree prediction in Europe by using five classes and
 283 a random forest classifier. Vieira et al. (2003) reported a $K = 0.77$ in eastern Amazon using seven
 284 classes and 1999 Landsat 7 ETM imagery. However, Sothe et al. (2017) reported K values of 0.98
 285 and 0.90 for respectively three successional forest stages and field in a subtropical forest in
 286 Southern Brazil by using Sentinel-2 and Landsat-8 data associated with the support vector machine
 287 algorithm. Kun et al. (2014) estimated K values of 0.70 to 0.85 for land-use type prediction
 288 (including forest) in China by using the support vector machine algorithm classifier and Landsat-
 289 8 images of rougher spatial resolution than Sentinel images. The very high accuracy of predictions
 290 by Kun et al. (2014) was probably due to the large-scale of the study and the clearly differentiated
 291 types of land considered.

292 **Relationship between presence of *P. monophylla* and environmental variables**

293 Ruggedness of the terrain was the most important topographic variable, significantly explaining
294 the presence of pines in Sierra La Asamblea (Table 3). Ruggedness, which is strongly positively
295 correlated with slope, may reduce solar radiation, air temperature and evapotranspiration due to
296 increased shading (Tsujino et al., 2006; Bullock et al., 2008). The ruggedness indicated by the TRI
297 index explains the presence of the pines because Sierra La Asamblea is heterogeneous in terms of
298 elevation. The VRM index was less important partly because the index is strongly dependent on
299 the vector aspect (Gisbert & Martí, 2010) and in the case of Sierra Asamblea the aspect is very
300 homogeneous and the index values therefore tend to be very low (Table 4), as also reported by Wu
301 et al. (2018). The pines were expected to colonize north facing slopes, which are exposed to less
302 solar radiation than slopes facing other directions. However, the topographical variable aspect was
303 not important in determining the presence of *P. monophylla* var. *californiarum* in the study site,
304 possibly because of physiological adaptations regarding water-use efficiency and photosynthetic
305 nitrogen-use efficiency (DeLucia & Schlesinger, 1991), as reported for the *Pinus monophylla*, *P.*
306 *halepensis*, *P. edulis* and *P. remota* in arid zones (Lanner & Van Devender, 2000; Helman et al.,
307 2017). The Mediterranean climate, with wet winters and dry summers, is another characteristic
308 factor in this mountain range. In the winter in this part of the northern hemisphere, the sun (which
309 is in a lower position and usually affects the southern aspect by radiation) is masked by clouds,
310 rainfall and occasional snowfall (León-Portilla, 1988). During the summer, the solar radiation is
311 more intense, but similar in all directions because the sun is closest to its highest point (Stage &
312 Salas, 2007).

313 The above-mentioned finding contrasts with those of other studies reporting that north-eastern
314 facing slopes in the northern hemisphere receive less direct solar radiation, thus providing more

315 favourable microclimatic conditions (air temperature, soil temperature, soil moisture) for forest
316 development, permanence and productivity than southwest-facing sites (Astrom et al., 2007; Stage
317 & Salas, 2007; Hang et al 2009; Marston et al., 2010; Klein et al., 2014). DeLucia & Schleinger
318 (1991) reported that *P. monophylla* populations in the Great Basin California desert with summer
319 rainfall (monsoon) preferred an east-southeast aspect with less intense solar radiation and
320 evapotranspiration.

321 The probability of occurrence of *P. monophylla* was also related to the climatic variable MTWM.
322 In Sierra La Asamblea, this pine species was found in a narrow range of MTWM of between 23.5°
323 and 25.2° (Table 1), which, however, is a smaller range than reported for the other pine species
324 (Tapias et al., 2004; Roberts & Ezcurra, 2012). Therefore, this species should adapt well to high
325 temperatures in the summer (Lanner et al., 2000), which is usually a very dry period in the study
326 site (León-Portilla, 1988). However, the probability of occurrence was greatest for an MTWM of
327 23.5°C (Table 4), which occurred at the top of Sierra La Asamblea, at an elevation of about 1,660
328 m). We therefore conclude that this species can also grow well when the MTWM is below 23.5°C.
329 On the other hand, considering MTWM as factor yielded a probability of occurrence of 25-80%.
330 The spatial resolution of the climatic data by the national database run by the University of Idaho
331 is probably not adequate for describing the microhabitat of *P. monophylla* (Rehfeldt et al., 2006;
332 Marston et al., 2010).

333 Identification of the *P. monophylla* stands in Sierra La Asamblea as the most southern populations
334 represents an opportunity for research on climatic tolerance and community responses to climatic
335 variation and change.

336 **ACKNOWLEDGEMENTS**

337 We are grateful to E. Espinoza, F. Macias and A. Guerrero for support with the fieldwork.

338 **REFERENCES**

339 Abraira V. 2001. El índice kappa. *Semergen* 27:247-249. DOI:10.1016/S1138- 3593(01)73955-X

340 Allen CD, Macalady AK, Chenchouni H, Bachelet D, Vennetier M, Kitzberger G, Rigling H,

341 Breshears D, Hoog T, Gonzalez PK., Fensham R, Zhangm Z, Castro J, Demidova N, Jong-

342 Hwan L, Allard G, Running S, Semerci A, Cobbt N. 2010. A global overview of drought

343 and heat-induced tree mortality reveals emerging climatic change risks for forest. *Forest*

344 *ecology and management* 259:660-684. DOI: 10.1016/j.foreco.2009.09.001.

345 Allouche, O., Tsoar, A., Kadmon, R., 2006. Assessing the accuracy of species distribution models:

346 Prevalence, kappa and the true skill statistic (TSS). *J. Appl. Ecol.* 43, 1223–1232.

347 DOI:10.1111/j.1365-2664.2006.01214.x

348 Bailey DK. 1987. A study of *Pinus* subsection *Cembroides*. The single-needle pinyons of the

349 Californias and the Great Basin. *Notes from the Royal Botanic Garden, Edinburgh.* 44:275-

350 310.

351 Borràs J, Delegido J, Pezzola A, Pereira M, Morassi G, Camps-Valls G. 2017. Land use

352 classification from Sentinel-2 imagery. *Revista de Teledetección* 48:55-66. DOI:

353 10.4995/raet.2017.7133.

354 Braspenning P J, Thuijsman F. 1995. Artificial neural networks: an introduction to ANN theory

355 and practice. Springer Science & Business Media. USA. 295 p.

- 356 Brockmann Consult, 2017. Sentinel Application Platform (SNAP). Available at:
357 <http://step.esa.int/main/> (accessed 18 April 2017).
- 358 Bullock SH, Heath D. 2006. Growth rates and age of native palms in the Baja California desert.
359 *Journal of Arid Environments* 67(3):391-402. DOI: 10.1016/j.jaridenv.2006.03.002.
- 360 Bullock SH, Salazar Ceseña JM, Rebman JP, Riemann H. 2008. Flora and vegetation of an isolated
361 mountain range in the desert of Baja California. *The Southwestern Naturalist* 53:61-73. DOI:
362 10.1894/0038-4909(2008)53[61:FAVOAI]2.0.CO;2.
- 363 Callaway RM, DeLucia EH, Nowak R, Schlesinger WH. 1996. Competition and facilitation:
364 contrasting effects of *Artemisia tridentata* on desert vs. montane pines. *Ecology* 77:2130-
365 2141. DOI: 10.2307/2265707.
- 366 Chambers JC. 2001. *Pinus monophylla* establishment in an expanding *Pinus-Juniperus* woodland:
367 Environmental conditions, facilitation and interacting factors. *Journal of Vegetation Science*
368 12:27-40.
- 369 CONABIO. 2017. Comisión Nacional para el Conocimiento y uso de la Biodiversidad. Geoportal
370 de información. Sistema Nacional de información sobre Biodiversidad. Available at:
371 <http://www.conabio.gob.mx/informacion/gis/> (accessed 12 February 2017).
- 372 Congalton RG. 1991. A review of assessing the accuracy of classifications of remotely sensed
373 data. *Remote sensing of environment* 37:35-46. DOI: 10.1016/0034-4257(91)90048-B
- 374 DeCastilho CV, Magnusson WE, de Araújo RNO, Luizao RC, Luizao FJ, Lima AP, Higuchi N.
375 2006. Variation in aboveground tree live biomass in a central Amazonian Forest: Effects of

- 376 soil and topography. *Forest ecology and management* 234:85-96. DOI:
377 10.1016/j.foreco.2006.06.024.
- 378 DeLucia, EH, & Schlesinger, WH. 1991. Resource-use efficiency and drought tolerance in
379 adjacent Great Basin and sierran plants. *Ecology*, 72(1), 51-58. DOI: 10.2307/1938901
- 380 Development Core Team. 2017. A language and environment for statistical computing. R
381 foundation for statistical computing, Vienna Austria. Available at: [http://www.R-](http://www.R-project.org)
382 [project.org](http://www.R-project.org). (accessed 8 September 2017).
- 383 Drusch M, Del Bello U, Carlier S, Colin O., Fernández V, Gascón F, Hoersch B, Isola C, Laberinti,
384 P, Martimort P, Meygret A, Spoto F, Sy O, Marchese F, Bargellini P. 2012. Sentinel-2:
385 ESA's Optical High-Resolution Mission for GMES Operational Services. *Remote sensing*
386 *environment* 120:25-36. DOI: 10.1016/j.rse.2011.11.026.
- 387 Elliott KJ, Miniati CF, Pederson N, Laseter SH. 2005. Forest tree growth response to hydroclimate
388 variability in the southern Appalachians. *Global Change Biology* 21(12):4627-4641. DOI:
389 10.1111/gcb.13045.
- 390 ESA, 2017. European Space Agency. Copernicus, Sentinel-2. Available At: <http://www.esa.int>
391 (accessed 21 March 2016).
- 392 Fawcett, T. 2006. An introduction to ROC analysis. *Pattern Recognition Letters* 27:861–874. DOI:
393 10.1016/j.patrec.2005.10.010

- 394 García E. 1998. Clasificación de Köppen, modificado por García, E. Comisión Nacional para el
395 Conocimiento y Uso de la Biodiversidad (CONABIO), 1998. Available at:
396 <http://www.conabio.gob.mx/informacion/gis/> (accessed 2 June 2017).
- 397 Gisbert FJG, Martí IC. 2010. Un índice de rugosidad del terreno a escala municipal a partir de
398 Modelos de Elevación Digital de acceso público. *Documento de Trabajo*. Available at:
399 https://wheui3.grupobbva.com/TLFU/dat/DT_7_2010.pdf
- 400 Goodchild MF. 1994. Integrating GIS and remote sensing for vegetation analysis and modeling:
401 methodological issues. *Journal of Vegetation Science* 5:615-626. DOI: 10.2307/3235878.
- 402 Guo PT, Wu W, Sheng QK, Li MF, Liu HB, Wang ZY. 2013. Prediction of soil organic matter
403 using artificial neural network and topographic indicators in hilly areas. *Nutrient cycling in*
404 *agroecosystems* 95:333344. DOI: 10.1007/s10705-013-9566-9.
- 405 Helman D, Osem Y, Yakir D, Lensky IM. 2017. Relationships between climate, topography, water
406 use and productivity in two key Mediterranean forest types with different water-use
407 strategies. *Agricultural and Forest Meteorology* 232:319-330. DOI:
408 10.1016/j.agrformet.2016.08.018.
- 409 Hepner G, Logan T, Ritter N, Bryant N. 1990. Artificial neural network classification using a
410 minimal training set. Comparison to conventional supervised classification.
411 *Photogrammetric Engineering and Remote Sensing* 56(4):469-473.
- 412 Immitzer M, Vuolo F, Atzberger C. 2016. First Experience with Sentinel-2 Data for Crop and Tree
413 Species Classifications in Central Europe. *Remote Sensing* 8:1-27. DOI: 10.3390/rs8030166.

- 414 INEGI. 2013. Conjunto de datos vectoriales de uso de suelo y vegetación escala 1:250 000, serie
415 V. Instituto Nacional de Estadística y Geografía. Aguascalientes. *Available at:*
416 <http://www.conabio.gob.mx/informacion/gis/> (accessed 10 September 2015).
- 417 Klein T, Hoch G, Yakir D, Körner C. 2014. Drought stress, growth and nonstructural carbohydrate
418 dynamics of pine trees in a semi-arid forest. *Tree physiology* 34:981-992. DOI:
419 10.1093/treephys/tpu071.
- 420 Kun J, Xiangqin W, Xingfa G, Yunjun J, Xianhong X, Bin L. 2014. Land cover classification
421 using Landsat 8 Operational Land Imager data in Beijing, China. *Geocarto International*
422 29:941-951. DOI:10.1080/10106049.2014.894586.
- 423 Lanner RM, Van Devender TR. 2000. The recent history of pinyon pines. In: Richardson, D. M.
424 (eds). *The American Southwest*, Cambridge University Press. 171–182
- 425 León-Portilla. 1988. Miguel del Barco, Historia natural y crónica de la antigua California.
426 Universidad Nacional Autónoma de México, México. 483 p.
- 427 Madonsela S, Cho MA., Ramoelo A, Mutanga O. 2017. Remote sensing of species diversity using
428 Landsat 8 spectral variables. *ISPRS Journal of Photogrammetry and Remote Sensing* 133:
429 116–127. DOI: 10.1016/j.isprsjprs.2017.10.008.
- 430 Marston, RA. 2010. Geomorphology and vegetation on hillslopes: interactions, dependencies, and
431 feedback loops. *Geomorphology*, 116(3-4), 206-217.
- 432 Moran RV. 1983. Relictual northern plants on peninsular mountain tops. In: *Biogeography of the*
433 *Sea of Cortez*; University of California Press, Berkeley, USA. 408–410.

- 434 Olofsson O, Foody GM, Stehman SV, Woodcock CE. 2013. Making better use of accuracy data
435 in land change studies: Estimating accuracy and area and quantifying uncertainty using
436 stratified estimation. *Remote Sensing of Environment* 129:122–131. DOI:
437 10.1016/j.rse.2012.10.031
- 438 Olofsson, P, Foody, GM, Herold, M, Stehman, SV, Woodcock, CE, Wulder, MA. 2014. Good
439 practices for estimating area and assessing accuracy of land change. *Remote Sensing of*
440 *Environment* 148, 42-57. DOI: 10.1016/j.rse.2014.02.015
- 441 Osem Y, Zangy E, Bney-Moshe E., Moshe Y, Karni N, Nisan Y. 2009. The potential of
442 transforming simple structured pine plantations into mixed Mediterranean forests through
443 natural regeneration along a rainfall gradient. *Forest Ecology Management* 259:14–23.
444 DOI:10.1016/j.foreco.2009.09.034.
- 445 Pettorelli N. 2013. The Normalized Difference Vegetation Index. Oxford, University Press. United
446 Kingdom. 194 p.
- 447 QGIS Development. 2016. QGIS Geographic Information System. Open source Geospatial
448 Foundation. Available at: <http://qgis.osgeo.org>
- 449 Radoux J, Chomé G, Jacques DC, Waldner F, Bellemans N, Matton N, Lamarche C, d’Andrimont
450 R, Defourny P. 2016. Sentinel-2’s potential for sub-pixel landscape feature detection.
451 *Remote Sensing* 8(6):488. DOI:10.3390/rs8060488.

- 452 Rehfeldt GE. A spline model of climate for the Western United States. 2006. Gen Tech Rep.
453 RMRS-GTR-165. U.S. Department of Agriculture, Forest Service, Rocky Mountain
454 Research Station, Fort Collins, Colorado, USA.
- 455 Rehfeldt GE, Crookston NL, Warwell MV, Evans JS. 2006. Empirical analyses of plant-climate
456 relationships for the western United States. *International journal plant science* 167:1123–
457 1150. DOI: 1058-5893/2006/16706-0005.
- 458 Richards JA. 1999. *Remote Sensing Digital Image Analysis*, Springer-Verlag, Berlin, p.240.
- 459 Riley SJ, Degloria SD, Elliot R. 1999. A terrain ruggedness index that quantifies topographic
460 heterogeneity. *Intermountain Journal of Sciences* 5:23–27
461 (<http://arcscrips.esri.com/details.asp?dbid=12435>).
- 462 Roberts N, Ezcurra E. Desert Climate. 2012. In: Rebman, JP, Roberts NC, ed. *Baja California*
463 *Plant Field Guide*. San Diego Natural History Museum. San Diego, USA. 1-23.
- 464 Rouse JW, Haas RH, Schell A, Deering DW. 1974. Monitoring vegetation systems in the Great
465 Plains with ERTS. Proceedings of the Third Earth Resources Technology Satellite-1
466 Symposium, December 10–15 1974, Greenbelt, MD, NASA, Washington, DC, pp.301–317.
- 467 Sáenz-Romero C, Rehfeldt GE, Crookston NL, Duval P, St-Amant R, Beaulieu J, Richardson BA.
468 2010. Spline models of contemporary, 2030, 2060 and 2090 climates for Mexico and their
469 use in understanding climate-change impacts on the vegetation. *Climatic Change*, 102:595-
470 623. DOI:10.1007/s10584-009-9753-5.

- 471 Salas EAL, Valdez R, Michel S. 2017. Summer and winter habitat suitability of Marco Polo argali
472 in southeastern Tajikistan: A modeling approach. *Heliyon* 3(11):e00445.
473 DOI:10.1016/j.heliyon.2017.e00445.
- 474 Sappington, JM., Longshore, KM., Thompson, D. B. 2007. Quantifying landscape ruggedness for
475 animal habitat analysis: a case study using bighorn sheep in the Mojave Desert. *Journal of*
476 *wildlife management*, 71(5):1419-1426. DOI: 10.2193/2005-723
- 477 Satage AR, Salas C. 2007. Interactions of Elevation, Aspect, and Slope in Models of Forest Species
478 Composition and Productivity. *Forest Science* 53:486-492. Available at:
479 <http://www.ingentaconnect.com/>
- 480 Silva-Flores R, Pérez-Verdín G, Wehenkel C. 2014. Patterns of tree species diversity in relation
481 to climatic factors on the Sierra Madre Occidental, Mexico. *PloS one* 9, e105034. DOI:
482 10.1371/journal.pone.0105034.
- 483 Shirk AJ, Waring K, Cushman S, Wehenkel C, Leal-Sáenz A, Toney C, Lopez-Sanchez CA. 2017.
484 Southwestern white pine (*Pinus strobiformis*) species distribution models predict large range
485 shift and contraction due to climate change. *Forest Ecology Management* (in review).
- 486 SNAP. 2017. ESA's Sentinel-toolbox ESA Sentinel Application Platform. Version 6.0.0.
- 487 Sothe C, Almeida CMD, Liesenberg V, Schimalski MB. 2017. Evaluating Sentinel-2 and Landsat-
488 8 Data to Map Successional Forest Stages in a Subtropical Forest in Southern Brazil. *Remote*
489 *Sensing* 9(8):838. DOI:10.3390/rs9080838.

- 490 Spasojevic MJ, Bahlai CA, Bradley BA, Butterfield BJ, Tuanmu MN, Sistla S, Wiederholt R,
491 Suding KN. 2016. Scaling up the diversity-resilience relationship with trait databases and
492 remote sensing data: the recovery of productivity after wildfire. *Global Change Biology*
493 22(4):1421–1432. DOI: 10.1111/gcb.13174.
- 494 Tapias R, Climent J, Pardos JA, Gil L. 2004. Life histories of Mediterranean pines. *Plant Ecology*
495 171: 53-68. DOI:10.1023/B:VEGE.0000029383.72609.f0.
- 496 Telespazio VEGA Deutschland GmbH 2016. Sentinel-2 MSI-Level-2A. Prototype Processor
497 Installation and User Manual. Available at:
498 <http://step.esa.int/thirdparties/sen2cor/2.2.1/S2PAD-VEGA-SUM-0001-2.2.pdf>
- 499 Tsujino R, Takafumi H, Agetsuma N, Yumoto T. 2006. Variation in tree growth, mortality and
500 recruitment among topographic positions in a warm temperate forest. *Journal of*
501 *Vegetation Science* 17:281-290. DOI:10.1658/1100-
502 9233(2006)17[281:VITGMA]2.0.CO;2.
- 503 Venables WN, Ripley BD. 2002. Modern Applied Statistics with S-Plus. Fourth Edition. New
504 York, Springer.
- 505 Vieira ICG, de Almeida AS, Davidson EA, Stone TA, de Carvalho CJR, Guerrero JB. 2003.
506 Classifying successional forests using Landsat spectral properties and ecological
507 characteristics in eastern Amazonia. *Remote Sensing of Environment* 87(4):470-481.
508 DOI:10.1016/j.rse.2002.09.002.

509 Wu W, Li AD, He XH, Ma R, Liu HB., Lv JK. 2018. A comparison of support vector machines,
510 artificial neural network and classification tree for identifying soil texture classes in
511 southwest China. *Computers and Electronics in Agriculture* 144:86-93. DOI:
512 10.1016/j.compag.2017.11.037.